

Solving Online Resource-Constrained Scheduling for Follow-Up Observation in Astronomy: a Reinforcement Learning Approach

Yajie Zhang^{1,2}, Ce Yu^{1,2,*}, Chao Sun^{1,2}, Jizeng Wei^{1,2}, Junhan Ju^{1,2}, Shanjiang Tang^{1,2}

Abstract

In the astronomical observation field, determining the allocation of observation resources of the telescope array and planning follow-up observations for targets of opportunity (ToOs) are indispensable components of astronomical scientific discovery. This problem is computationally challenging, given the online observation setting and the abundance of time-varying factors that can affect whether an observation can be conducted. This paper presents ROARS, a reinforcement learning approach for online astronomical resource-constrained scheduling. To capture the structure of the astronomical observation scheduling, we depict every schedule using a directed acyclic graph (DAG), illustrating the dependency of timing between different observation tasks within the schedule. Deep reinforcement learning is used to learn a policy that can improve the feasible solution by iteratively local rewriting until convergence. It can solve the challenge of obtaining a complete solution directly from scratch in astronomical observation scenarios, due to the high computational complexity resulting from numerous spatial and temporal constraints. A simulation environment is developed based on real-world scenarios for experiments, to evaluate the effectiveness of our proposed scheduling approach. The experimental results show that ROARS surpasses 5 popular heuristics, adapts to various observation scenarios and learns effective strategies with hindsight.

Keywords:

Online scheduling, astronomical follow-up observation, reinforcement learning, resource-constrained project scheduling.

1. Introduction

Astronomical sky surveys, the primary avenue for exploring the universe, have generated numerous scientific breakthroughs [1, 2]. Observation scheduling constrained by time-varying observation conditions and shared limited resources is a crucial problem for survey observation, using a telescope array with multiple telescopes. The visibility of celestial objects changes in real time and the lifetime of expensive astronomical observation equipment is limited [3]. So efficient observation scheduling and resource management are conducive to maximizing scientific output. Making follow-up observations for targets of opportunity (ToOs) in sky surveys refers to gathering additional data to further understand specific transient phenomena of great scientific interest identified during the initial survey [4]. It requires the use of various instruments and specific filters as astronomers are committed to unveil more details, enhancing the comprehensive exploration of the cosmos.

The complexity of the astronomical observation task scheduling problem has been proved to be NP-hard [5]. The difficulty of solving resource-constrained task scheduling for online follow-up observations optimally is rooted in its intricate

nature. In the process of time-domain sky survey, it is a kind of closed-loop scheduling to deal with ToOs that appear suddenly. The multi-band follow-up scheduling algorithm needs to deal with the uncertainty of resource availability (including observable time limited by observation conditions, telescope filters, etc.), target properties (arrival time, duration, and requirements for observation band, exposure time and observation mode), etc. Note that these target priority constraints are determined by astronomers for scientific discovery after the target appears, and there are no prior probability distributions. Specifically, incoming follow-up observation targets have various precedence relations and observation band requirements, often requiring simultaneous observations by multiple telescopes with different filters across bands, as illustrated in Fig. 1. As the Earth rotates, the visibility of each target changes over time. The observation time window of the target is affected by the positions of the observation sites and the target and changes with time, which is an important computational challenge in our scheduling problem. Through observation sites that distributed around the world, different ToOs can be coordinated observation. Careful consideration of execution order and time-varying constraints is essential for coordinated and timely observations. In distributed telescope array environment, the variance in available observation time across sites, coupled with potential competition for target observations due to their distribution, presents greater challenges to the execution of observation plans [6]. The majority of these issues are addressed using integer linear programming (ILP) and meticulously designed heuristics. For exam-

*Corresponding author.

Email addresses: zyj0928@tju.edu.cn (Yajie Zhang), yuce@tju.edu.cn (Ce Yu)

¹College of Intelligence and Computing, Tianjin University, No.135 Yaguan Road, Haihe Education Park, Tianjin 300350, China

²Technical R&D Innovation Center, National Astronomical Data Center, No.135 Yaguan Road, Haihe Education Park, Tianjin 300350, China

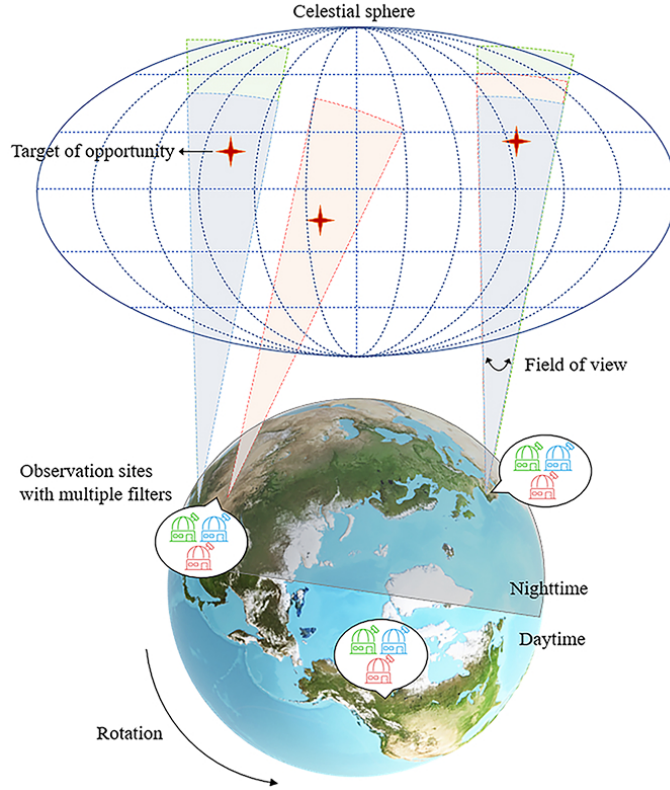


Figure 1: Conceptual illustration of distributed telescope array follow-up observation for targets of opportunity.

ple, the Zwicky Transient Facility allocates survey fields to time blocks, minimizing the need for filter changes and ensuring precise control over the number of exposures per field [7]. Similar optimization objectives are considered for the Large Synoptic Survey Facility using genetic algorithms [8]. Moreover, heuristic methods are widely employed for solving this problem within the astronomical field, e.g., lowest airmass [9], smallest telescope slew angle [10], for finding optical counterparts to transients. However, for practical large-scale survey observation, determining when and where to apply these heuristics, and establishing their prioritization, is both inflexible and time-consuming. In addition, meta-heuristic algorithm has been used for agile earth observation satellite scheduling problem [11], but there are significant differences in the observation modes of satellites and telescopes.

Revisiting the above challenges, given the problem scale and computational complexity, we investigate the use of reinforcement learning (RL) approaches for this real-world resource-constrained scheduling problem. RL benefits from abundant training data generated by repetitive scheduling decisions in astronomical observation systems, allowing for effective learning. Meanwhile, RL has the capability to model intricate systems and decision-making strategies through deep neural networks, akin to the architectures employed for gaming agents [12]. This is achieved by integrating various input signals to enable online application in stochastic environments [13]. However, the application of RL-based scheduling to astronomical observation domains is not straightforward given the lack of well-suited

model and benchmark. The processing of high-priority follow-up tasks and the efficient generation of observation plans during the survey are essential to the guarantee of astronomical discoveries. Therefore, as the key to developing effective observation resource allocation plans, the effective acquisition astronomical observation knowledge and observation modeling are pressing issues that demand urgent attention.

To our knowledge, the combination of online resource management, astronomical follow-up ToO observation and telescope array is not considered in the literature so far. So in this paper we contribute by, first, defining and modeling the real-world resource-constrained scheduling problem in telescope array setting, considering both multiple telescopes in one observation site (we call intra-site) and geographically distributed in multiple sites. Second, we propose a new approach to tackle the problem using deep reinforcement learning (DRL), named ROARS, for a Reinforcement learning approach for Online Astronomical Resource-Constrained Scheduling. A directed acyclic graph (DAG) is used to extract the problem-specific knowledge and model the temporal dependency of the problem. High quality solutions with different sizes and structures are learned by iteratively refining [14] existing solutions towards optimality using DRL. Because the approach of obtaining a complete solution directly from scratch, as employed in previous similar works [13, 15, 16], becomes challenging to achieve feasibility when scaling up the observation scheduling. Here we focus on online setting where the follow-up observation tasks arrive dynamically with unpredictable constraints and cannot be

preempted once scheduled. The proposed ROARS is evaluated through extensive simulations performed on real-world data. Our preliminary results show that ROARS is able to generate solutions of consistent quality in various astronomical observation scenarios, thereby facilitating robust and rapid schedule adaptation amidst uncertainty. The quality of schedules generated by ROARS can exceed those of the heuristic baselines and offline scheduling scenarios, where the entire observation task sequence is known prior to scheduling. The approach can also be extended to distributed telescope array observation environments with robustness performance.

2. Related Work

Resource scheduling and optimization problems, pervasive and fundamental issues in complex system, have been extensively studied from both theoretical and empirical perspectives [17, 18]. There are numerous studies demonstrating effective use of DRL in several real-world resource scheduling scenarios, such as smart manufacturing [19], city-wide firefighting [20], steel production [21, 22], resource provisioning in Internet of Things ecosystem [23, 24], logistics and retail [21]. Existing studies demonstrate that RL exhibits effectiveness in terms of the solution quality, and can achieve substantial time savings compared to the classical heuristic approaches [25]. Therefore, DRL is extensively investigated as an effective approach for controlling complex systems.

Despite the clear need, there is an absence of research undertaken in the area of intelligent astronomical observation resource allocation for telescope array. Nowadays, resource allocation and management methods in most astronomical survey observation projects can be divided into two types, based on ILP algorithms [26, 27] and human-generated heuristics [4]. Nevertheless, with the increase of the number of telescopes and observation targets, especially in the environment of telescope array observation, fine-scale observation strategy optimization requires extensive manual intervention, which exceeds the ability of conventional planning algorithms and classical solvers. For the observation environment using a distributed telescope array, a flexible multilevel global scheduling model is proposed for a generic telescope array scheduling problem by Zhang et al. [3]. While their algorithm produces long-term scheduling solutions in survey observation mode, it does not undertake precise resource coordination for follow-up observations of ToOs. Jia et al. implements a telescope array observation simulator and applies DRL into a space debris observation scenario [6]. But since publication, there is currently no established general approach for resource management in online follow-up astronomical observation using an array of multiple telescopes.

The follow-up observation scheduling problem in astronomy can be seen as a special resource-constrained project scheduling problems (RCPSP [28]). In order to achieve the robust scheduling [29, 30], researchers propose multiple heuristic and meta-heuristic procedures to allocate time buffers in a given schedule while ensuring adherence to a predefined project due date [31]. By contrast, inserting time buffers in a proactive way

to deal with scheduling uncertainties is not in line with the principle of telescopic observation, because the telescope is expensive and has limited life, observation time is a very valuable resource. Li et al. develop efficient approximate dynamic programming (ADP) algorithms for RCPSP with uncertain task duration, using constraint programming and a hybrid ADP framework to enhance performance and efficiency [32]. Brvcic et al. address the issue of inflexibility in proactive-reactive scheduling by introducing threshold-based cost functions for deviation penalties in projects with stochastic task duration [33]. While Xie et al. focus on RCPSP with uncertain resource availability [34], they use a new Markov decision process model and a rollout-based ADP algorithm, significantly improving performance over heuristic methods. Compared with these traditional problems, the problem of RCPSP in time-domain survey to be solved in this paper focuses more on fast processing of special targets to ensure their observation quality, rather than maintaining the stability of the original tasks.

With the development of deep learning technology in recent years, one research [13] presents an example solution that transforms the problem of packing tasks with diverse resource demands into a learning problem. The resource allocation strategies are directly learned from experience. However, it only considers a single-cluster situation, and factors such as the dependency between jobs have not been investigated. Another research [35] relies on the graph neural network to address RCPSP of varying sizes, including in presence of uncertain task duration. Cai et al. further solves the RCPSP with resource disruptions, and uses proximal policy optimization (PPO) to train the model in an end-to-end way for performance optimization [36]. Their work is relevant for us, but for the follow-up observation scenario in astronomical domain, scheduling strategies should consider real locations of telescopes, distributions of observation targets, and filter requirements. The constrained observation conditions are closely related to these time-varying factors. Therefore, the current industrial scheduling methods are difficult to be directly applied in the field of astronomical observation.

In other recent work, the local rewriting is proposed for combinatorial optimization [14], the performance is assessed across three distinct domains: online job scheduling, expression simplification, and vehicle routing. It has shown better performance than heuristics using multiple metrics in solving complex problems where generating an entire solution directly is challenging. Given its effectiveness in capturing hierarchical and sequential structures, and order constraints [37], the Child-Sum Tree-LSTM architecture is well-suited for the dynamic and complex nature of resource scheduling in astronomical observations. So it is clear that despite a lack of exploration into a general intelligent resource management approach in the astronomical observation domain, the existence of mature and extensive research supports the exploration as a feasible approach for tackling the application challenges.

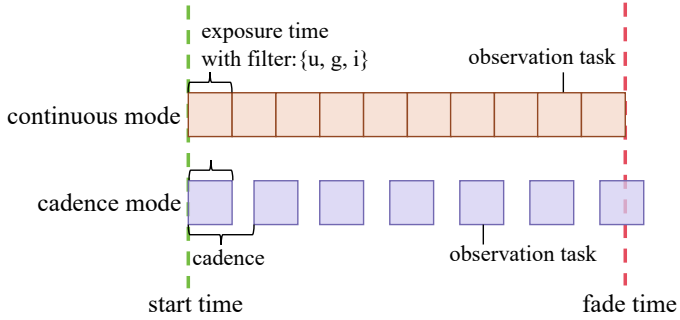


Figure 2: Schematic diagram of the relationship between the follow-up observation target and observation task. We give the division of a target of opportunity that arises during a sky survey into multiple follow-up observation tasks (i.e., multiple exposures) according to its observational requirements in continuous observation mode or cadence observation mode. As an example, this follow-up target requires simultaneous observations in the u,g,i three bands.

3. Follow-up observation scheduling in astronomy

In this section, the problem setting and parameters are presented first, followed by its MDP formulation, which lays the foundation for our ROARS algorithm to be developed in the succeeding sections.

3.1. Problem statement

Formally, the resource-constrained scheduling problem for follow-up observations in astronomy can be defined by a tuple (M, N, R) where: M represents a set of ToOs that have been identified for key follow-up observations; N is a set of observation sites, which can include one or multiple geographically distributed observation sites, each equipped with multiple telescopes; R is a set of resource types, which represents the types of observation bands (filters) configured at each site. Detailed parameter descriptions and notations are presented in Table 1. We suppose to have an astronomical observation environment with d types of filters. All sites have a full set of filters R , each telescope providing one. Tasks with different filters can overlap on the same site, maximizing telescope resource use.

Table 2 demonstrates the defined set of properties of the incoming ToOs for follow-up observations during sky survey. For target i , a d -dimensional vector F_i denotes the filter requirement of the various filter types. The priority (property #7) flags the urgency and importance of the observation target. Property #3 and #4 reflect the required start and end monitoring time of the follow-up observation of the target object, during which multiple shots at different times should be taken according to the required exposure time. Here, Property #6 considers two modes of observation that are common in astronomical observation, observations of one need to follow immediately on from one another (cannot overlap), while observations of another have gaps of required cadence between them. Depending on the exposure time for target i (denoted as E_i) required for different celestial objects, astronomers need to take multiple shots before they disappear. Each exposure of a specific sky region constitutes an observation task. Fig. 2 shows an example of how a follow-up observation object can be divided into multiple observation tasks (i.e., exposures) based on multiple properties.

Note that the follow-up observation monitoring for target i , can be performed by a group of observation tasks K with different numbers according to its required single exposure time. Each observation task j of target i can be specified as $v_j = (f_i, A_j, e_i)$. It is worth noting that the band requirements and exposure time are the same for each exposure (i.e. observation task) of each target, so f_j and E_j are equal to f_i and E_i respectively. A_j denotes the required beginning observation time of task j . We assume that the above properties of each follow-up target is known upon arrival, and are not dependent on the site. Note that in this paper, ToOs are preprocessed, divided into observation tasks based on the observation mode. We operate under the assumption that observation tasks arrive at the telescope array in real-time, at discrete intervals. A waiting task queue is available, capable of accommodating up to W tasks. When a new follow-up observation task is received, it can be promptly assigned or added to a queue. If the queue reaches its capacity, scheduling the new task requires the immediate execution of at least one task in the waiting queue to accommodate the incoming task. W can be adjusted based on the practical observation scale. Additionally, we assume a fixed filter requirement throughout the entire execution of the observation tasks, with no allowance for preemption.

3.2. Observation impact factors

There are various of time-varying features that influence the feasibility and quality of the observation. This paper utilizes airmass [38] as the evaluation metric to determine whether a telescope is suitable for observing a target. The airmass measures the atmospheric thickness through which astronomical light passes before reaching the telescope, which is influenced by zenith angle, altitude, atmospheric conditions, and etc. Lower airmass observations are preferred in astronomy for better image quality and less atmospheric distortion [9]. Meanwhile, the optical radiation from the sun will also affect the resolution and clarity of the observations to some extent, so the sun's position and radiation need to be taken into account as well. The relative location of the observation site and the target, and the observation time determine the astronomical observation conditions, which vary with time. Hence, these spatial and temporal constraints significantly increase the computational cost of resource allocation calculations.

3.3. MDP formulation

Therefore, the follow-up observation scheduling for ToOs can be modeled as an MDP with the following components.

3.3.1. Stages

The decision stages are the time periods at which observation scheduling decisions are made. Let t denote the time period (stage) and T be the set of all time periods.

3.3.2. States

State of the system S_t encompasses all relevant information at decision stage t . According to the above assumptions and definitions, the states of the system at any time t can be defined

Table 1: Summary of key parameters and variables.

Notation	Description
Set of targets of opportunity (ToOs)	$M = \{i_1, i_2, \dots, i_m\}$
Celestial coordinates of target i	$C_i = (\alpha_i, \delta_i)$
Scientific value or priority of target i	V_i
Set of observation sites	$N = \{s_1, s_2, \dots, s_n\}$
Geographic coordinates of site s	$L_s = (\phi_s, \lambda_s)$
Set of observation bands (filters) available	$R = \{b_1, b_2, \dots, b_d\}$
Required observation bands (filters) of target i	$F_i = \{f_1, f_2, \dots, f_d\}$
Required exposure time e_b in band b for target i	$E_i = \{(b, e_b) \mid b \in F_i\}$
Set of tasks for target i based on observation mode	$K = \{j_1, j_2, \dots, j_k\}$
Required beginning observation time of task j	A_j
Scheduled beginning observation time of task j	B_j

Table 2: Properties of the incoming ToOs in follow-up observation scenarios.

Property ID	Name	Description
#1	Target coordinate	Right ascension and declination are used to uniquely identify the location coordinates of the target.
#2	Filter requirement	Denote the observation filters of telescopes need to be used simultaneously to capture multi-band information.
#3	Start time	The time required to start the follow-up monitoring of the target.
#4	Fade time	The time required to end the follow-up monitoring of the target.
#5	Exposure time	The requirement of the observation target for single exposure time.
#6	Observation mode	Information on whether observations need to follow immediately on from one another, or monitor a target every few minutes/hours.
#7	Priority	Denote the urgency or importance of the observation target.

by: current time t , the current time in the scheduling horizon, current availability of observation sites, visibility window and observation quality of tasks, exposure requirements.

3.3.3. Decisions

At each decision stage, the following decisions need to be made (defined as the solution): target selection, which observation task j to observe, which site s to use for the observation, **and when to start the observation** B_j . So it can be formulated by a binary decision variable $x_{s,j,f,t} \in \{0, 1\}$ indicating whether site s is assigned to observe task j in band f at time t .

3.3.4. Astronomical objectives and cost function

Swiftly addressing the incoming follow-up observation tasks in astronomical science is crucial for timely capturing transient celestial events and phenomena. Because the rapid response enables scientists to gather critical data, facilitating real-time analysis and enhancing the chances of making groundbreaking discoveries in the dynamic and evolving cosmos. Therefore, we adopt the *average task slowdown* as the primary optimization objective. Formally, for each observation task j of target i , it can be defined as:

$$\eta_j = \frac{C_j - A_j}{E_i}, \quad (1)$$

where A_j and B_j denote the required beginning observation time and scheduled beginning observation time, respectively. And

$C_j = B_j + E_i$ is the task completion time. The objective function to minimize the sum of slowdowns for all tasks can be written as:

$$\min \sum_{j \in K} \eta_j = \min \sum_{j \in K} \frac{(B_j + E_i) - A_j}{E_i} \quad (2)$$

Normalizing the completion time by the observation task's exposure time mitigates potential bias towards lengthy observations, a situation that may arise when optimizing for objectives like mean completion time. The value of η is ≥ 1 . Therefore, our focus is on developing a schedule that minimizes the overall task slowdown by assigning follow-up ToO observations to telescopes equipped with the necessary filters, while adhering to the constraints of observation conditions. That means to get B_j closer to A_j , the slowdown η closer to 1.

The cost-to-go function $J_t(S_t)$ represents the minimum expected cost from stage t to the end of the planning horizon, given the current state S_t . Based on the decision $x_{s,j,f,t}$, the state transition function describes how the state evolves from S_t to S_{t+1} can be formulated as $f(S_t, x_{s,j,f,t})$. The immediate cost $g(S_t, x_{s,j,f,t})$ represents the cost incurred at stage t due to decision $x_{s,j,f,t}$. The cost-to-go function at stage t is recursively defined as the immediate cost plus the expected cost-to-go from the next stage onward [39]:

$$J_t(S_t) = \min_{x_{s,j,f,t}} \left[g(S_t, x_{s,j,f,t}) + \mathbb{E}[J_{t+1}(S_{t+1}) | S_t, x_{s,j,f,t}] \right] \quad (3)$$

Here, the immediate cost $g(S_t, x_{s,j,f,t})$ can be interpreted as the slowdown incurred by the decision at stage t :

$$g(S_t, x_{s,j,f,t}) = \eta_{i,j} = \frac{(B_{i,j} + E_{i,j}) - A_{i,j}}{E_{i,j}} \quad (4)$$

So by optimizing the model, we define the scheduling problem of multi-band follow-up observation for the occurrence of ToOs in the time-domain survey of astronomical telescope arrays. The goal of the model is to minimize the task slowdown, and the cost function is described by the recursive formula of the state and decision stage, which provides a comprehensive framework for scheduling.

4. A RL approach: ROARS

4.1. Graph representation

Based on the above problem definition, the online resource-constrained follow-up observation scheduling problem is solved by a reinforcement learning based approach named ROARS, depicted in Fig. 3. Each schedule is depicted as a DAG, illustrating the interdependence of observation task scheduling times. In this representation, each observation task v_j corresponds to a node in the DAG of scheduling, with an additional node v_0 representing the observation telescope. If an observation task v_j is scheduled upon arrival at time A_j (i.e., $B_j = A_j$), we include a directed edge $\langle v_0, v_j \rangle$ in the graph. Alternatively, there must exist at least one task $v_{j'}$ such that $C_{j'} = B_j$ (meaning task j begins immediately after task j'). We include an edge $\langle v_{j'}, v_j \rangle$ for each such task $v_{j'}$ in the graph.

For the follow-up observation task embedding, in intra-site telescope array setting with D kinds of resources (filters), we embed each task into a vector of dimension $(D \times (E_{max} + 1) + 1)$. Here, E_{max} represents the maximum exposure duration for an observation task. For distributed telescope array, it will be a $(N \times D \times (E_{max} + 1) + 1)$ -dimensional vector, N denotes the number of observation sites. This vector encodes details about task attributes and the observation site's status during task execution. The specifics of the task embedding are outlined below. Consider a task $v_j = (\rho_j, A_j, E_i)$ for target i . We represent the total resources utilization across all takes at each time step t as $\rho'_t = (\rho'_{t1}, \rho'_{t2}, \dots, \rho'_{tD})$. Taking intra-site observations as an example, each observation task v_j is represented as a $(D \times (E_{max} + 1) + 1)$ -dimensional vector, where the first D dimensions of the vector are ρ_j , representing its observation resource requirement. The $D \times E_i$ dimensions of the vector are the concatenation of $\rho'_{B_j}, \rho'_{B_j+1}, \dots, \rho'_{B_j+E_i-1}$, which describes the utilization of the observation resources during the execution of the task v_j . Specifically, when the energy consumption E_i is less than the maximum allowed energy E_{max} , the subsequent $D \times (E_{max} - E_j)$ dimensions are set to zero. The final dimension of the embedding vector signifies the task's slowdown in the current schedule. Each task v_j is represented by its embedding denoted as e_j . Additionally, the embedding of the observation telescope, denoted as v_0 , is represented by a zero vector, $e_0 = 0$. It can be seen from Fig. 3 that two possible observation task schedules and their corresponding graph

Algorithm 1 Algorithm of a Single Rewriting Step

Input: Current observation task v_j , another task $v_{j'}$, and the dependency graph representation of task schedule s_t

Output: The dependency graph representation of task schedule in next time step s_{t+1}

```

1: if  $C_{j'} < A_j$  or  $C_{j'} == B_j$  then
2:   return  $s_t$ 
3: end if
4: if  $j' \neq 0$  then
5:    $B'_j = C_{j'}$ 
6: else
7:    $B'_j = A_j$ 
8: end if
9:  $C'_j = B'_j + E_j$ 
10:  $J =$  all tasks in  $s_t$  except  $v_j$  that are scheduled within
     $[B'_j, C'_j]$ 
11: Sort  $J$  in the topological order
12: for  $v_p \in J$  do
13:    $B'_p =$  the earliest time that task  $v_p$  can be scheduled
14:    $C'_p = B'_p + E_p$ 
15: end for
16: for  $v_p \notin J, B'_p = B_p, C'_p = C_p$  do
17:    $s_{t+1} = \{(B'_p, C'_p)\}$ 
18: end for
19: return  $s_{t+1}$ 

```

representations may be generated. Node 0 denotes the beginning of the scheduling process, with additional instances added for multiple observation telescopes. Scheduling 2 is superior to scheduling 1 because there is no slowdown, i.e., all 3 tasks can be observed at the required observation start time (i.e. $B = A$), ensuring maximum scientific monitoring.

We expand upon the Child-Sum Tree-LSTM architecture introduced in [40] to encode the schedule graphs. For a job v_j , let $(h_1, c_1), (h_2, c_2), \dots, (h_p, c_p)$ denote the LSTM states of all parent nodes of v_j , so its LSTM state can be represented as:

$$(h, c) = \text{LSTM} \left(\left(\sum_{i=1}^p h_i, \sum_{i=1}^p c_i \right), e_j \right). \quad (5)$$

4.2. Model specification and rewriting

After constructing the graph representation, we train a neural-based policy to iteratively refine the current scheduling solution by locally rewriting parts of it until convergence. This approach draws inspiration from [14]. We employ the end-to-end reinforcement learning to train the policy, encouraging the cumulative enhancement of the solution. For the telescope observation scheduling problem, finding a feasible solution that meets the constraints of observation time and geographical location is straightforward. Additionally, the search space displays favorable local structures that facilitate incremental enhancements to the solution. Thus, a comprehensive solution offers a contextual basis for enhancement through a rewriting-based approach, facilitating the computation of additional features, a challenge when generating a solution from scratch. Various solutions

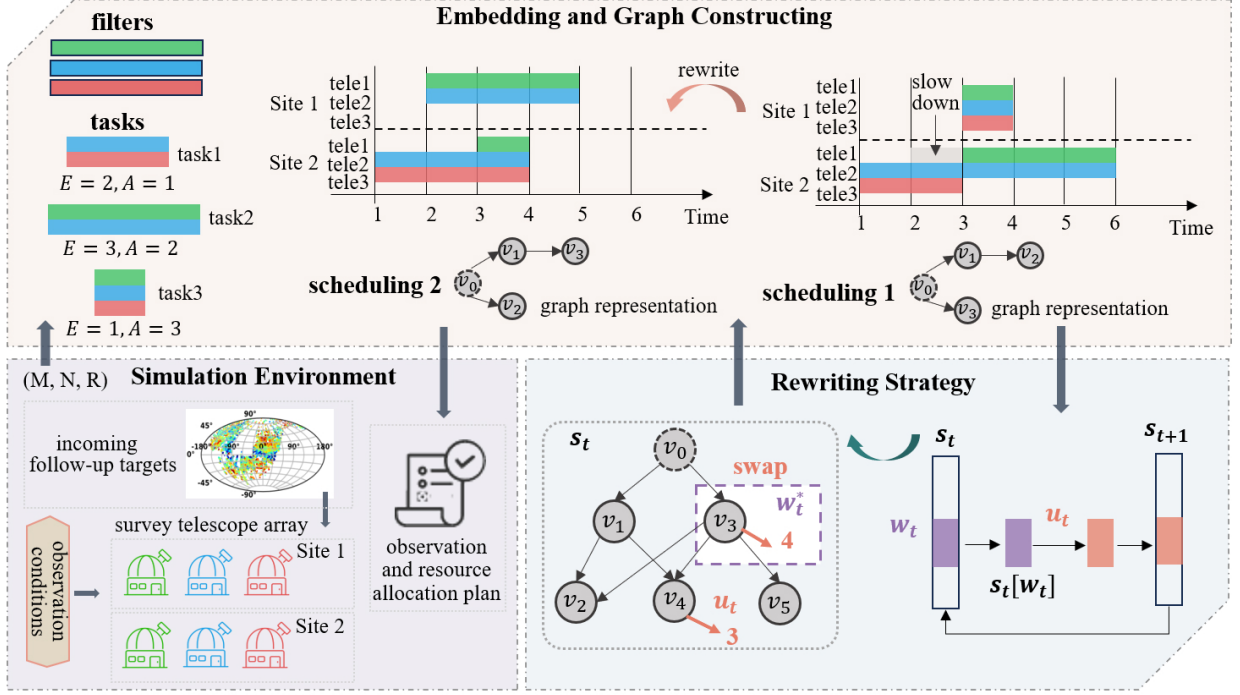


Figure 3: An illustrative example of ROARS. By parsing incoming follow-up targets from the astronomical observation simulation environment, the scheduling algorithm completes resource allocation and outputs the observation plan to each observation site. We give an illustration of the rewriting optimization strategy and an example of two potential task schedules at a single observation site and their corresponding graphical representations.

may converge towards optimization through a shared pathway, which could be encapsulated as local rewriting rules. Furthermore, straightforward rules such as task swapping could enhance performance. These aspects enable the application of the rewriting formulation to diverse instances of follow-up observation scheduling. We can train the neural network to investigate relationships among diverse solutions within the search space. Our rewriting strategy incorporates a region-selection policy and a rule-selection policy.

Each solution represents a state, and every local region, along with its corresponding rewriting rule, acts as an action. Algorithm 1 describes steps for a single rewriting. The rewriting rules involve relocating the present task v_j to be positioned as a child of another job v_j or v_0 within the graph. This results in scheduling observation task v_j to commence either after task v_j concludes or at its arrival time A_j . As depicted in Fig. 3, s_t represents the dependency graph of the observation task schedule. Each circle with an index greater than 0 denotes a task node, while node 0 serves as an additional representation of the observation site. The graph's edges denote the observation dependencies among follow-up tasks. The region-picking policy chooses a task ω_t from all task nodes for rescheduling, while the rule-picking policy determines a movement action u_t for ω_t . Afterwards, s_t is modified to obtain a new dependency graph s_{t+1} .

Let \mathcal{U} be the rewriting rule set, shown in Fig. 3. Assume that s_t represents the current solution (or state) at iteration t . Firstly, a state-dependent region set $\Omega(s_t)$ is computed, which is problem-dependent, and covers all follow-up observation task

nodes for scheduling. We then select a region $\omega_t \in \Omega(s_t)$ using the region-picking policy $\pi_\omega(\omega_t | s_t)$. For each $\omega_t \in \Omega(s_t)$, we calculate a score $Q(s_t, \omega_t)$, which reflects the potential benefit of rewriting. A higher score suggests that rewriting $s_t[\omega_t]$ may be advantageous.

Afterwards, a rewriting rule u_t is selected for the region ω_t using the rule-picking policy $\pi_u(u_t | s_t[\omega_t])$, where $s_t[\omega_t]$ denotes a subset of the state s_t . The chosen rewriting rule $u_t \in \mathcal{U}$ is then applied to $s_t[\omega_t]$, resulting in the subsequent state represented as $s_{t+1} = f(s_t, \omega_t, u_t)$. The rewriting sequence in the forward pass can be denoted as

$$s_T = (s_0, (\omega_0, u_0)), (s_1, (\omega_1, u_1)), \dots, (s_{T-1}, (\omega_{T-1}, u_{T-1})). \quad (6)$$

Hence, commencing with an initial solution (or state) s_0 , our aim is to discover a sequence of rewriting steps s_T that minimizes the final cost $c(s_T)$.

Note that we both use fully connected neural networks for the prediction of region score and selection of a rewriting rule.

4.3. Training details

Our region-picking policy π_ω and rule-picking policy π_u are trained in the meantime. The reward function of training can be defined as $r(s_t, (\omega_t, u_t)) = c(s_t) - c(s_{t+1})$. For π_ω , we express the parameterization as a softmax function of the $Q(s_t, \omega_t; \theta)$:

$$\pi_\omega(\omega_t | s_t; \theta) = \frac{\exp(Q(s_t, \omega_t; \theta))}{\sum_{\omega_t} \exp(Q(s_t, \omega_t; \theta))} \quad (7)$$

The training of $Q(s_t, \omega_t; \theta)$ involves aligning it with the cumulative reward obtained from the present learning policies π_ω and

π_u :

$$L_\omega(\theta) = \frac{1}{T} \sum_{t=0}^{T-1} \left(\sum_{t'=t}^{T-1} \gamma^{t'-t} r(s'_t, (\omega'_t, u'_t)) - Q(s_t, \omega_t; \theta) \right)^2 \quad (8)$$

Here, T represents the episode length, indicating the count of rewriting steps, while γ signifies the decay factor. Regarding the rule-picking policy, we employ the advantage actor-critic mechanism, leveraging $Q(s_t, \omega_t; \theta)$ as the critic. This approach mitigates bootstrapping-related issues that may arise from sample insufficiency and training instability. The advantage function can be represented as:

$$\Delta(s_t, (\omega_t, u_t)) \equiv \sum_{t'=t}^{T-1} \gamma^{t'-t} r(s'_t, (\omega'_t, u'_t)) - Q(s_t, \omega_t; \theta) \quad (9)$$

The loss function of the rule selector can be represented as:

$$L_u(\phi) = - \sum_{t=0}^{T-1} \Delta(s_t, (\omega_t, u_t)) \log \pi_u(u_t | s_t[\omega_t]; \phi) \quad (10)$$

Moreover, we denote the overall loss function as $L(\theta, \phi) = L_u(\phi) + \alpha L_\omega(\theta)$, where α serves as a hyperparameter.

During the training process, α is set to 10. The numbers of region picking and rule picking are both 15 for intra-site telescope array, while both 30 for distributed array, which are sufficient for figuring out a competitive scheduling solution. The hyperparameter specifying the total number of rewriting steps is set to 100 iterations. For all tasks in our evaluation, suppose the probability of re-sampling the region for rewriting is $1 - p_c$, p_c starts with a initial value of 0.5, and is gradually decayed by 0.8 every 1000 time steps until it reaches a minimum value of 0.01, at which point it remains constant. We set the decay factor for the cumulative reward to $\gamma = 0.9$, and the initial learning rate to $1e-4$, which is then decayed by a factor of 0.9 every 1000 time steps. Furthermore, we maintain a fixed batch size of 128 during training. The model is optimized using the Adam, with all weights initialized uniformly randomly within the range of $[-0.1, 0.1]$.

5. Experiment

The tested algorithms were implemented in Python. In our evaluation, the neural networks are implemented using PyTorch [41]. All implementation and experiments were performed on an Ubuntu server featuring a 4-core Intel Xeon CPU (clocked at 2.2 GHz), 32 GB of memory, and a Tesla V100 GPU.

5.1. Setup

We conduct experiments on simulated data based on various scenarios in real-life settings to investigate the effectiveness of ROARS in terms of solution quality, computational speed, robustness and scalability. We develop a simulator environment to model the observations of both intra-site and distributed telescope arrays, including the diverse conditions, telescope states,

and follow-up targets for telescope arrays to test the algorithm under varied settings. These conditions act as constraints, aiding in determining available resources for a target at a given time. **As shown in Fig. 4, we select 5 real observation sites worldwide to simulate the formation of the telescope array. The position of the ToOs are generated from 100 sky fields with the configuration parameters described later. In addition, we simulate the arrival of ToOs within 4 hours. Since different ToOs have varying observation requirements and need to be monitored over a period of time, the generated instances are based on a collection of observation tasks according to the duration and exposure time required by the ToOs.** The simulator serves for both model training and evaluation. Note that the coordinate of the targets and observation sites are collected from real observations. According to the configuration of the real telescope array under construction, we use u , g and i bands as possible filter requirement inputs. In addition, We generated one hundred thousand follow-up observation task sequences randomly, allocating 80% for training and reserving 10% each for validation and testing. The waiting task queue length, denoted as W , is fixed at 10. Initial schedules were generated using the *First Come First Serve* (FCFS) method, known for its low overhead during construction.

5.1.1. Evaluation metric.

According to the actual astronomical observation needs, we utilize the *average task slowdown* $\eta_j \equiv (C_j - A_j)/E_j$ as the evaluation metric. It is preferred that follow-up observation tasks be handled as soon as possible after arrival.

5.1.2. Task properties.

In order to adequately test the robustness and generalization of ROARS, various observation task properties are evaluated: (1) *Average arrival rate of ToOs*: the probability of a new ToO arrival, the *Steady* task frequency sets it to be 10% (because normally targets that need to be followed up in the sky survey observation are in the minority), and *Dynamic* task frequency indicates that the ToO arrival rate varies randomly at each time step; (2) *Duration of the follow-up observation*: the time from the beginning when the opportunity target requires observation monitoring to the end, *Long* for the time duration requirement of the target is in $[120, 240]$ minutes, *Short* for $[60, 119]$ minutes, and *Non-uniform* task duration; (3) *Resource distribution*: observation tasks might have different resource requirements, we consider *Uniform* resource as the ToO selects two of the three possible resources with the same probability to observe simultaneously, while *Non-uniform* refers to simultaneous observations of one, two or three of bands required with 10%, 20% and 30% probability, respectively; (4) *Single exposure time*: length of each observation task, *Long* means single exposure time is in $[10, 20]$ minutes, *Short* for $[1, 9]$ minutes, and *Non-uniform* exposures; (5) *Observation mode*: the two ways to make a series of sequential observations in astronomy, one is to perform observations that follow immediately on from one another (*Exposure count*), the other is to monitor the target with required *Cadence*.

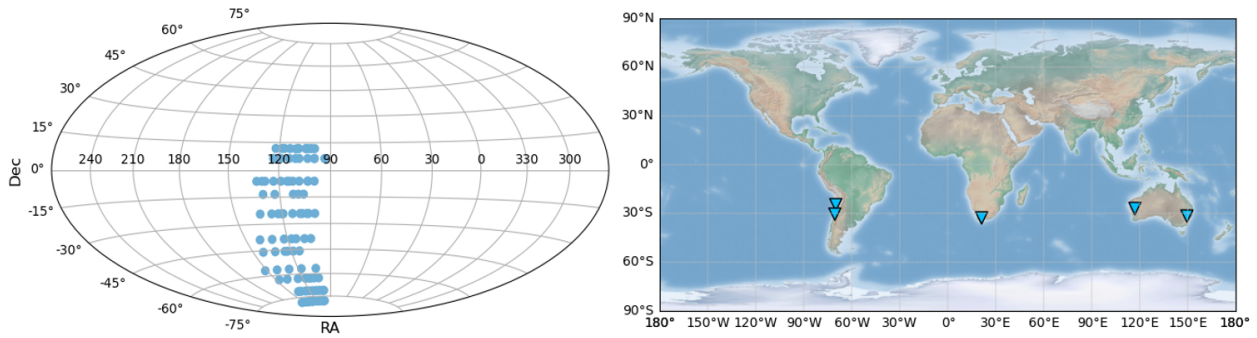


Figure 4: The location information of observation sites and fields in dataset generation.

5.1.3. Baselines on heuristics.

For intra-site telescope array scenarios, we implement 5 online heuristic approaches that are popular in existing machine scheduling and RCPSP problems for comparison. *Shortest Task First* (STF) allocates the tasks with the shortest exposure time in the waiting task queue at each time step. *First Come First Serve* (FCFS) schedules each observation task in the increasing order based on the arrival time. *Earliest Due Date* (EDD) schedules the observation tasks with the earliest end time. *Shortest Processing Time* (SPT) prioritizes targets with the shortest duration (from the time required to start monitoring to its fade) to be monitored. And *Resource Intensity Priority* schedules the target with the highest resource requirements first. In this paper, resource demand intensity is defined as the number of required observation resource types multiplied by the total exposures. In addition, we have also tried to employ the optimal solver (e.g. Gurobi [42] and CBC [43]) for the problem in this context, but both seem intractable in general. Therefore, we omit the comparison.

For scenarios of distributed observation sites, heuristically obtaining a feasible solution is more complicated. It involves two steps of selecting the follow-up task and selecting the site, so we correspondingly design the following baselines. We make heuristic site selections based on *equipment priority factor* and *observation quality*, which are what astronomers tend to do in the current study. In practical observations, the *equipment priority factor* for each site is usually related to the weather changes, which can be predicted or obtained in real time. Here we use the airmass of each schedule to represent the *observation quality*, while generate the *equipment priority factor* of each site randomly as input. It should be noted that ROARS has not been specifically optimized for these two parameters. The heuristic baselines are *Shortest Task best Quality site First* (SQTF), *Shortest Task best Priority site First* (SPTF), *First come Task best Quality site First* (FQTF), *First come Task best Priority site First* (FPF), *shortest Processing best Quality site First* (PQTF), *shortest Processing best Priority site First* (PPTF), *earliest Due Task best Quality site First* (DQTF), *earliest Due Task best Priority site First* (DPTF), *Shortest Task best Quality site First* (RQTF), and *Shortest Task best Priority site First* (RPTF).

5.1.4. Baselines on offline scheduling.

In order to evaluate the effectiveness of these algorithms, we examine an offline scenario where the complete task sequence is known beforehand. This is equivalent to simulating an unbounded waiting task queue. This setting, with additional prior knowledge, serves as a strong baseline for evaluation. We utilize STF-offline, a basic heuristic approach that schedules tasks in ascending order of duration.

5.2. Result comparison

Table 3: Statistics of solution quality compared to baselines in terms of average slowdown and computation time.

	Avg. slowdown	Time (s)
STF	16.47	0.11
FCFS	27.23	0.01
EDD	23.59	0.12
SPT	15.49	0.08
RIP	25.93	0.13
Offline	7.82	0.19
ROARS	7.34	0.08

Our first experiment compares the solution quality in terms of the average slowdown and computation time, as demonstrating in Table 3. In this experiment, training and testing instances are with steady task frequency, observation mode with cadence, non-uniform duration of follow-up task observation (20% long, 80% short), non-uniform resource distribution, and non-uniform single exposure time (20% short, 80% long). We conduct the experiments on one thousand different instances and average the results. It can be seen that ROARS outperforms both online heuristic baselines and the offline approach. It is more time-efficient than STF, EDD, and Offline. For the solution quality, ROARS can achieve nearly a 50% improvement compared to STF and SPT, which are the better performing heuristics. The average slowdown of Offline approach is comparable to that of ROARS, but is much more time-consuming. The Offline approach takes the knowledge of the entire incoming task sequence into account, which is helpful but costs larger time for analysis.

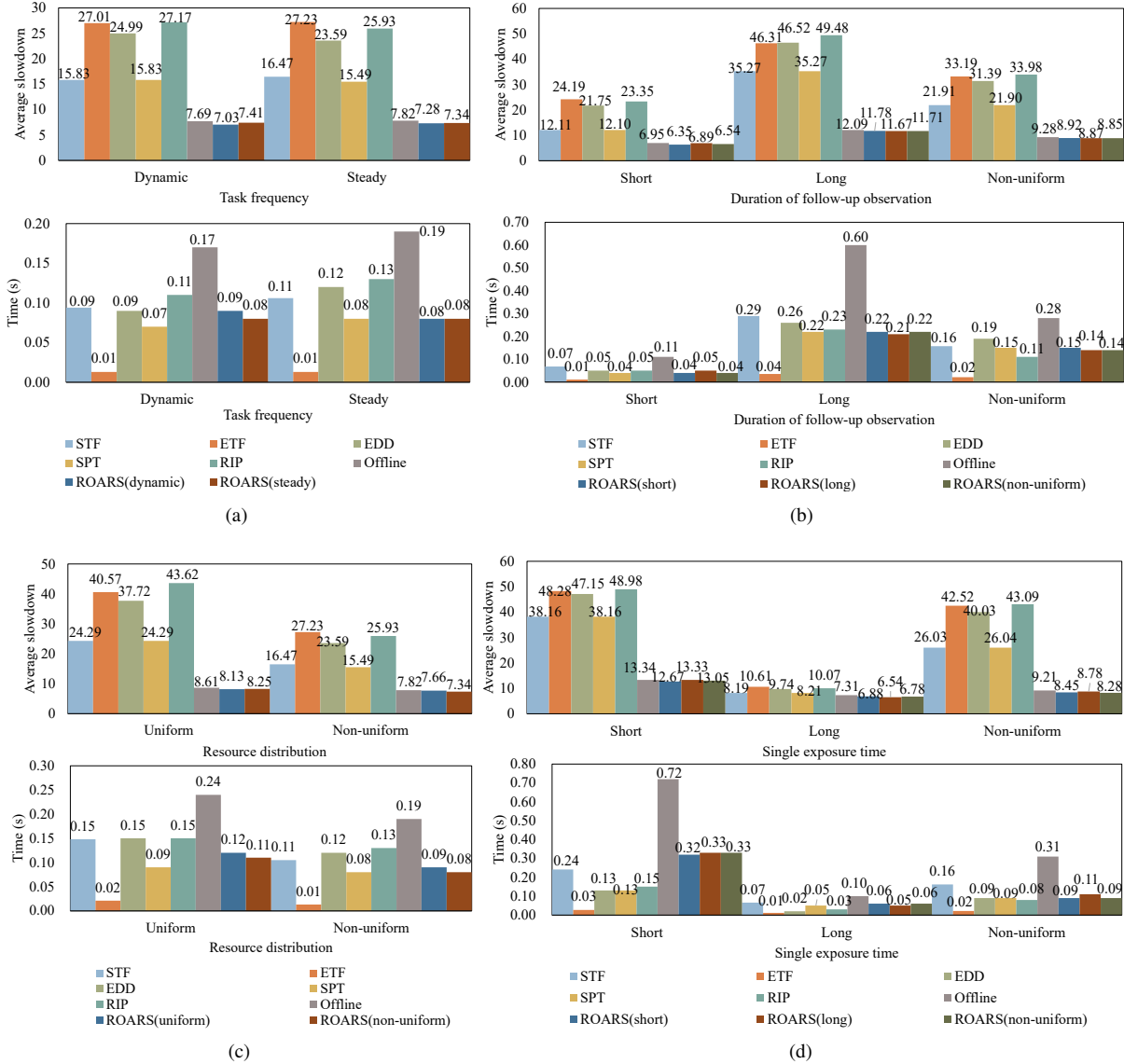


Figure 5: Experimental results of ROARS varying the following task properties: (a) task frequency of the incoming ToOs; (b) duration of follow-up observation; (c) resource distribution; and (d) single exposure time. Except for the influence of the properties to be explored on the results, the remaining properties in each experiment are set to be the same as those in the experiment presented in Table 3.

5.2.1. Results on generalization of various distributions.

Our second experiment evaluates the proposed ROARS on different distributions of the incoming ToO observation tasks. As shown in Fig. 5, we perform ablation experiments in different scenarios for each property. We can observe that for the average slowdown, ROARS is superior to all various input distributions. When we set all single exposure time of observation tasks long, STF and OffLine show acceptable performance, similar to ROARS. This is because for the same observation task duration, the longer the single exposure time, the fewer observations need to be performed, and the difficulty of solving the calculation decreases. Therefore, it illustrates that the proposed ROARS can deal with more complicated scenarios and the solutions obtained are more effective when extended to larger scale problems. In addition, ROARS can exhibit robust generalization to distributions not encountered during training, demonstrating the efficacy of local rewriting rules. Leveraging local context proves advantageous, yielding solutions with broader applicability, aligning with our design principles.

Furthermore, Fig. 6 demonstrates the effectiveness and robustness of ROARS when generalizing to different observation modes. In the field of astronomical observation, due to the rotation of the Earth, the effect of tasks implementing observations at different times varies greatly. The experimental results indicate that our proposed ROARS can effectively adapt to different observation modes and efficiently generate scheduling schemes based on observable times.

5.2.2. Extended to distributed telescope array.

Table 4: Statistics of solution quality compared to baselines in distributed observation environment. Results are compared in terms of average slowdown and computation time.

	Avg. slowdown	Time (s)
SQTF	11.75	0.24
FQTF	23.28	0.13
SPTF	13.75	0.22
FPTF	20.91	0.03
PQTF	14.75	0.09
PPTF	16.67	0.09
DQTF	23.77	0.12
DPTF	24.89	0.14
RQTF	24.00	0.15
RPTF	26.02	0.18
Offline	5.16	1.26
ROARS	4.89	0.22

Moreover, we extend the ROARS to the environment of distributed telescope array observation. This means that for the same observation target, the observation sites have appropriate observation resources at different times. The same setting for the observation task properties are adopted as experiments for single site scenario. Table 4 presents the results comparisons to heuristic algorithms (including selecting tasks and sites heuristically). Due to more sufficient observation resources, the overall slowdown is reduced compared with results of the intra-site telescope array observations, indicating that multiple sites

cooperate to process the coming follow-up tasks. On the contrary, distributed observation resources also increase the computational complexity of the problem, resulting in longer computing time. It can be observed that the *Shortest Task First* heuristics lead to a better overall slowdown than the other heuristics, while *Resource Intensity Priority* performs the worst. This may be due to the different time windows and visibility constraints of different observation targets, leading to resource competition and saturation. Prioritizing tasks with high resource intensity may not be able to complete other tasks in the optimal time window, resulting in a decrease in overall efficiency. Compared with the static heuristic method, our DRL-based method can constantly adjust the strategy according to the real-time observation data during the learning process to adapt to the changes in the environment and the dynamic needs of tasks, and optimize the long-term returns. Our results improved by 5.2% compared to offline algorithms that presume knowledge of the entire task sequence, further underscoring the effectiveness of ROARS. Note that the modeling of site priority and its impact on distributed scheduling results will be further explored.

6. Conclusion

In this paper, we have presented ROARS, an online scheduling approach for resource-constrained follow-up observation problem in astronomy. Our approach relies on modeling each schedule as a DAG which is encoded using extended Child-Sum Tree-LSTM architecture, and iteratively refining an existing solution towards optimality using deep reinforcement learning. Our proposed algorithm is validated and proven effective through numerical simulations conducted with real-world scenarios. Experimental results show that ROARS can infer schedules on unseen instances of higher quality than those produced by popular heuristics and even the offline setting, in various astronomical observation settings.

Furthermore, we will investigate the enhancement of solving capabilities by improving the model structure, especially in how to learn implicit competition for observation targets between the distributed observation sites. Moreover, now we use fully connected neural networks for region selection and rule selection, providing the flexibility to replace them with more advanced neural network models for further performance enhancement. ROARS can also be extended to other complex variants of dynamic resource management problems in astronomical observation domain, such as multi-objectives, more complex observation modes, etc. Our approach is designed for the ongoing deployment of the global telescope array for sky survey observations, serving as a crucial component in this initiative. Further experimentation is currently underway for the integration and refinement into the practical observation environment.

CRedit authorship contribution statement

Yajie Zhang: Conceptualization, Writing – original draft, Writing – review & editing, Visualization, Software, Validation.

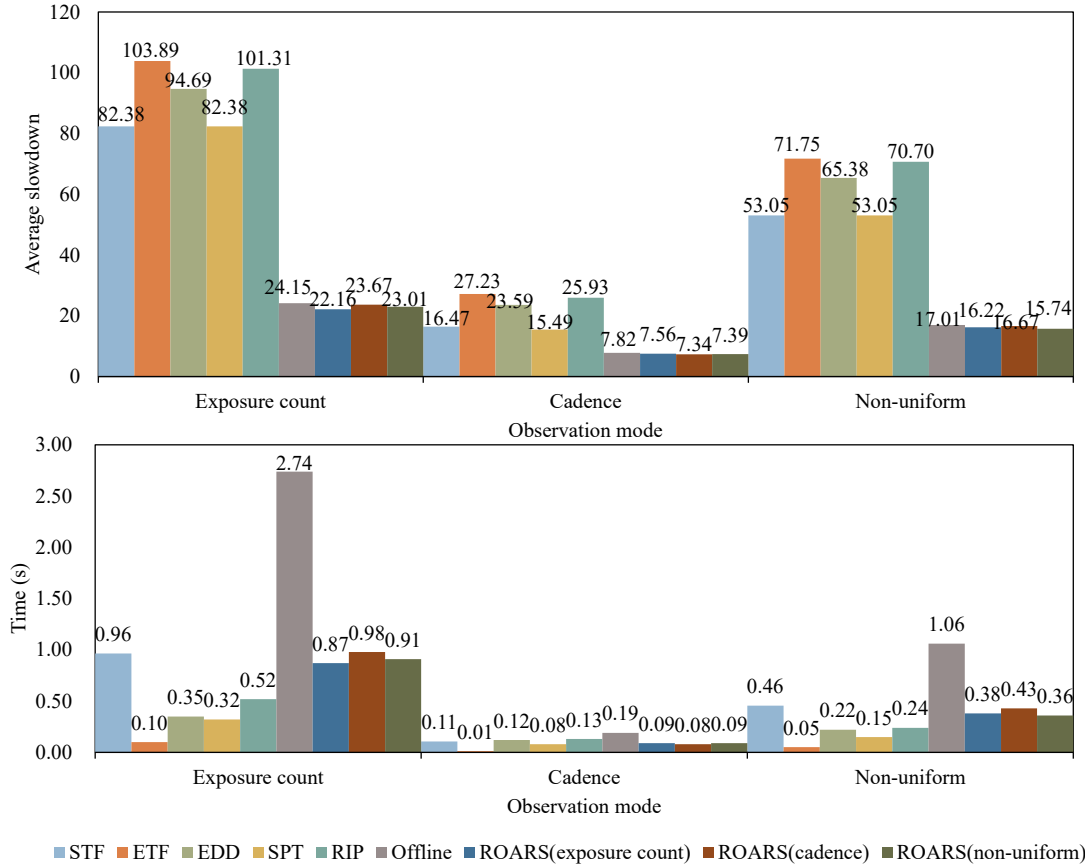


Figure 6: Experimental results of ROARS varying the observation modes.

Ce Yu: Supervision, Project administration, Funding acquisition. **Chao Sun:** Methodology, Validation, Funding acquisition. **Jizeng Wei:** Funding acquisition, Writing – review & editing. **Junhan Ju:** Writing – review & editing, Visualization, Data curation, Validation. **Shanjiang Tang:** Formal analysis, Methodology, Writing – review & editing.

Declaration of competing interest

The authors declare that they have no known competing financial interests or personal relationships that could have appeared to influence the work reported in this paper.

Data availability

Domain models and problem instances used in this paper can be provided by the authors upon request.

Acknowledgements

This work was financially supported by National Key R&D Program of China No. 2023YFA1608301 and the National Natural Science Foundation of China (NSFC) No. 12133010 and No. 12273025.

References

- [1] B. Ma, Z. Shang, Y. Hu, K. Hu, Y. Wang, X. Yang, M. C. Ashley, P. Hickson, P. Jiang, Night-time measurements of astronomical seeing at dome a in antarctica, *Nature* 583 (7818) (2020) 771–774.
- [2] T. Santana-Ros, M. Micheli, L. Faggioli, R. Cennamo, M. Devogèle, A. Alvarez-Candal, D. Oszkiewicz, O. Ramírez, P.-Y. Liu, P. G. Benavidez, et al., Orbital stability analysis and photometric characterization of the second earth trojan asteroid 2020 xl5, *Nature Communications* 13 (1) (2022) 447.
- [3] C. S. Z. S. Y. H. H. Z. J. Y. Yajie Zhang, Ce Yu, S. Tang, A multilevel scheduling framework for distributed time-domain large-area sky survey telescope array, *The Astronomical Journal* 165 (3) (2023) 77. doi:10.3847/1538-3881/acac24.
- [4] Q. Liu, P. Wei, Z.-H. Shang, B. Ma, Y. Hu, Research on scheduling of robotic transient survey for antarctic survey telescopes (ast3), *Research in Astronomy and Astrophysics* 18 (1) (2018) 005.
- [5] R. Bonvallet, A. Hoffstadt, D. Herrera, D. López, R. Gregorio, M. Al-muna, R. Hiriart, M. Solar, A methodological proposal for the development of an hpc-based antenna array scheduler, *Software and Cyberinfrastructure for Astronomy* 7740 (2010) 782–792.
- [6] P. Jia, Q. Jia, T. Jiang, J. Liu, Observation strategy optimization for distributed telescope arrays with deep reinforcement learning, *The Astronomical Journal* 165 (6) (2023) 233.
- [7] E. C. Bellm, S. R. Kulkarni, T. Barlow, U. Feindt, M. J. Graham, A. Goobar, T. Kupfer, C.-C. Ngeow, P. Nugent, E. Ofek, et al., The zwicky transient facility: Surveys and scheduler, *Publications of the Astronomical Society of the Pacific* 131 (1000) (2019) 068003.
- [8] E. Naghib, P. Yoachim, R. J. Vanderbei, A. J. Connolly, R. L. Jones, A framework for telescope schedulers: with applications to the large synoptic survey telescope, *The Astronomical Journal* 157 (4) (2019) 151.
- [9] J. Rana, S. Anand, S. Bose, Optimal search strategy for finding transients

- in large-sky error regions under realistic constraints, *The Astrophysical Journal* 876 (2) (2019) 104.
- [10] J. Rana, A. Singhal, B. Gadre, V. Bhalerao, S. Bose, An enhanced method for scheduling observations of large sky error regions for finding optical counterparts to transients, *The Astrophysical Journal* 838 (2) (2017) 108.
- [11] J. Wu, F. Yao, Y. Song, L. He, F. Lu, Y. Du, J. Yan, Y. Chen, L. Xing, J. Ou, Frequent pattern-based parallel search approach for time-dependent agile earth observation satellite scheduling, *Information Sciences* 636 (2023) 118924.
- [12] D. Silver, A. Huang, C. J. Maddison, A. Guez, L. Sifre, G. Van Den Driessche, J. Schrittwieser, I. Antonoglou, V. Panneershelvam, M. Lanctot, et al., Mastering the game of go with deep neural networks and tree search, *nature* 529 (7587) (2016) 484–489.
- [13] H. Mao, M. Alizadeh, I. Menache, S. Kandula, Resource management with deep reinforcement learning, in: *Proceedings of the 15th ACM workshop on hot topics in networks*, 2016, pp. 50–56.
- [14] X. Chen, Y. Tian, Learning to perform local rewriting for combinatorial optimization, *Advances in Neural Information Processing Systems* 32 (2019).
- [15] O. Vinyals, M. Fortunato, N. Jaitly, Pointer networks, *Advances in neural information processing systems* 28 (2015).
- [16] W. Kool, H. van Hoof, M. Welling, Attention, learn to solve routing problems!, *International Conference on Learning Representations* (2019).
- [17] S. Hartmann, D. Briskorn, An updated survey of variants and extensions of the resource-constrained project scheduling problem, *European Journal of operational research* 297 (1) (2022) 1–14.
- [18] Y. Liu, L. Huang, X. Liu, G. Ji, X. Cheng, E. Onstein, A late-mover genetic algorithm for resource-constrained project-scheduling problems, *Information Sciences* 642 (2023) 119164.
- [19] L. Wang, X. Hu, Y. Wang, S. Xu, S. Ma, K. Yang, Z. Liu, W. Wang, Dynamic job-shop scheduling in smart manufacturing using deep reinforcement learning, *Computer networks* 190 (2021) 107969.
- [20] S. Iqbal, R. Costales, F. Sha, Alma: Hierarchical learning for composite multi-agent tasks, *Advances in Neural Information Processing Systems* 35 (2022) 7155–7166.
- [21] L. Zhou, C. Lin, Z. Cao, Reinforcement-learning-based adaptive iterated local search approach to integrated order batching and job assignment problems in a smart warehouse: Driving growth for logistics and retail, *IEEE Robotics & Automation Magazine* 30 (2) (2023) 34–45. doi:10.1109/MRA.2023.3265515.
- [22] L. Feng, J. Peng, Z. Huang, Gas system scheduling strategy for steel metallurgical process based on multi-objective differential evolution, *Information Sciences* 654 (2024) 119817.
- [23] A. Chowdhury, S. A. Raut, H. S. Narman, Da-drls: Drift adaptive deep reinforcement learning based scheduling for iot resource management, *Journal of Network and Computer Applications* 138 (2019) 51–65.
- [24] H. Tran-Dang, S. Bhardwaj, T. Rahim, A. Musaddiq, D.-S. Kim, Reinforcement learning based resource management for fog computing environment: Literature review, challenges, and open issues, *Journal of Communications and Networks* 24 (1) (2022) 83–98.
- [25] N. Mazyavkina, S. Sviridov, S. Ivanov, E. Burnaev, Reinforcement learning for combinatorial optimization: A survey, *Computers & Operations Research* 134 (2021) 105400.
- [26] S. Lampoudi, E. Saunders, J. Eastman, An integer linear programming solution to the telescope network scheduling problem, *CoRR* abs/1503.07170 (2015). arXiv:1503.07170.
- [27] M. Solar, P. Michelon, J. Avarias, M. Garcés, A scheduling model for astronomy, *Astronomy and Computing* 15 (2016) 90–104.
- [28] E. L. Demeulemeester, W. Herroelen, W. S. Herroelen, *Project scheduling: a research handbook*, Vol. 49, Springer Science & Business Media, 2002.
- [29] O. Lambrechts, E. Demeulemeester, W. Herroelen, A tabu search procedure for developing robust predictive project schedules, *International Journal of Production Economics* 111 (2) (2008) 493–508.
- [30] O. Lambrechts, E. Demeulemeester, W. Herroelen, Time slack-based techniques for robust project scheduling subject to resource uncertainty, *Annals of operations Research* 186 (2011) 443–464.
- [31] S. Van de Vonder, E. Demeulemeester, W. Herroelen, Proactive heuristic procedures for robust project scheduling: An experimental analysis, *European Journal of Operational Research* 189 (3) (2008) 723–733.
- [32] H. Li, N. K. Womer, Solving stochastic resource-constrained project scheduling problems by closed-loop approximate dynamic programming, *European Journal of Operational Research* 246 (1) (2015) 20–33.
- [33] M. Brčić, M. Katić, N. Hlupić, Planning horizons based proactive rescheduling for stochastic resource-constrained project scheduling problems, *European Journal of Operational Research* 273 (1) (2019) 58–66.
- [34] F. Xie, H. Li, Z. Xu, An approximate dynamic programming approach to project scheduling with uncertain resource availabilities, *Applied Mathematical Modelling* 97 (2021) 226–243.
- [35] F. Teichteil-Königsbuch, G. Pováda, G. G. de Garibay Barba, T. Luchterhand, S. Thiébaux, Fast and robust resource-constrained scheduling with graph neural networks, *Proceedings of the International Conference on Automated Planning and Scheduling* 33 (1) (2023) 623–633.
- [36] H. Cai, Y. Bian, L. Liu, Deep reinforcement learning for solving resource constrained project scheduling problems with resource disruptions, *Robotics and Computer-Integrated Manufacturing* 85 (2024) 102628.
- [37] X. Yu, G. Li, C. Chai, N. Tang, Reinforcement learning with tree-lstm for join order selection, *2020 IEEE 36th International Conference on Data Engineering (ICDE)* (2020) 1297–1308.
- [38] F. Kasten, A. T. Young, Revised optical air mass tables and approximation formula, *Applied optics* 28 (22) (1989) 4735–4738.
- [39] R. Bellman, Dynamic programming, *Science* 153 (3731) (1966) 34–37. arXiv:https://www.science.org/doi/pdf/10.1126/science.153.3731.34, doi:10.1126/science.153.3731.34. URL https://www.science.org/doi/abs/10.1126/science.153.3731.34
- [40] K. S. Tai, R. Socher, C. D. Manning, Improved semantic representations from tree-structured long short-term memory networks, *Proceedings of the Annual Meeting of the Association for Computational Linguistics* (2015) 1556–1566doi:10.3115/v1/P15-1150.
- [41] A. Paszke, S. Gross, S. Chintala, G. Chanan, E. Yang, Z. DeVito, Z. Lin, A. Desmaison, L. Antiga, A. Lerer, Automatic differentiation in pytorch (2017).
- [42] I. Gurobi Optimization, *Gurobi optimizer reference manual*, Gurobi Optimizer Reference Manual (2014).
- [43] J. Forrest, R. Lougee-Heimer, *Cbc user guide*, Emerging theory, methods, and applications (2005) 257–277.